Rare Met. (2015) 34(11):770–775
DOI 10.1007/s12598-013-0124-z

RARE METALS
www.editorialmanager.com/rmet

Microstructure and thermoelectric properties of $Bi_{0.5}Na_{0.02}Sb_{1.48-x}In_xTe_3$ alloys fabricated by vacuum melting and hot pressing

Xing-Kai Duan*, Kong-Gang Hu, Da-Hu Ma,
Wang-Nian Zhang, Yue-Zhen Jiang,
Shu-Chao Guo

Received: 22 March 2013 / Revised: 4 April 2013 / Accepted: 26 July 2013 / Published online: 31 August 2013

Abstract The $Bi_{0.5}Na_{0.02}Sb_{1.48-x}In_xTe_3$ alloys ($x = 0.02–0.20$) were synthesized by vacuum melting and hot pressing methods at 753 K, 60 MPa for 30 min. Effects of Na and In dual partial substitutions for Sb on the thermoelectric properties were investigated from 300 to 500 K. Substituting Sb with Na and In can enhance the Seebeck coefficient effectively near room temperature. The electrical resistivity of the Na and In dual-doping samples is higher within the whole test temperature range. The $Bi_{0.5}Na_{0.02}Sb_{1.48-x}In_xTe_3$ samples ($x = 0.02$, 0.06) play a great role in optimizing the thermal conductivity. As for the $Bi_{0.5}$ $Na_{0.02}Sb_{1.46}In_{0.02}Te_3$ alloy, the minimum value of thermal conductivity reaches 0.53 $W{\cdot}m^{-1}{\cdot}K^{-1}$ at 320 K. The thermoelectric performance of the Na and In dual-doped samples is greatly improved, and a figure of merit *ZT* of 1.26 is achieved at 300 K for the $Bi_{0.5}Na_{0.02}Sb_{1.42}$ $In_{0.06}Te_3$, representing 26 % enhancement with respect to $ZT = 1.0$ of the undoped sample.

Keywords Microstructure; Dual doping; Hot pressing; Thermal conductivity; Thermoelectric properties

1 Introduction

Thermoelectric devices attracted a considerable amount of attention due to their ability of quietly converting waste heat from different sources into electricity or electrical power directly into cooling and heating [1–3]. The performance of thermoelectric materials can be defined by the dimensionless figure of merit $ZT = (S^2/\rho\kappa)T$, where S is the Seebeck coefficient, ρ is the electrical resistivity, κ is the thermal conductivity and T is the absolute temperature [4]. A good thermoelectric material requires a large Seebeck coefficient, low electrical resistivity and low thermal conductivity. Bi_2Te_3-based alloys are the most important commercial thermoelectric devices near room temperature. In recent years, the fabrication and thermoelectric properties of Bi_2Te_3-based alloys have been investigated by many researchers. For instance, utilizing hydrothermal synthesis, ball milling, rapid solidification and melt spinning, combining hot pressing (HP) [5–7], spark plasma sintering (SPS) [8–10], evacuated- and-encapsulated sintering [11], high-pressure sintering [12], hot extrusion [13], and nanocomposites [14–17] successfully introduced into bulk materials and relatively high thermoelectric performances of Bi_2Te_3-based alloys have been achieved.

Enhancement of the figure of merit is challenging because of the interdependence of physical parameters that define it. It is well known that doping can alter thermoelectric properties of the materials. It is certainly possible that more improvement is achieved based on the appropriately doped Bi_2Te_3-based alloys [18–21]. The In with substitution of three valence electrons for Sb with five valence electrons in the $Bi_{0.5}Sb_{1.5}Te_3$ alloy can be expected to be beneficial to the optimization of the carrier concentration, which results in an improvement of electrical conductivity. Moreover, alkali metal doping can effectively improve TE performance [22]. Up to now, few efforts were made to investigate the dual-doped Bi_2Te_3-based alloys. To study the feasibility of the dual doping in improving thermoelectric properties of the Bi_2Te_3-based bulk materials, a preliminary work on Na and In dual partial substitutions for

X.-K. Duan*, K.-G. Hu, D.-H. Ma, W.-N. Zhang, Y.-Z. Jiang, S.-C. Guo
Center for New Energy Materials Research, School of Mechanical and Materials Engineering, Jiujiang University, Jiujiang 332005, China
e-mail: duanxingkai@163.com

Sb in the $Bi_{0.5}Na_{0.02}Sb_{1.48-x}In_xTe_3$ alloys was carried out. In this paper, the $Bi_{0.5}Na_{0.02}Sb_{1.48-x}In_xTe_3$ ($x = 0.02$–0.20) and the $Bi_{0.5}Sb_{1.5}Te_3$ samples were fabricated by vacuum melting combining with hot-pressing method. The influences of Na and In dual doping on thermoelectric properties were investigated.

2 Experimental

Elemental powders of Bi (99.99 %), Sb (99.99 %), Te (99.99 %), Na (99.5 %) and In (99.99 %) were weighed in the atomic ratios of $Bi_{0.5}Sb_{1.5}Te_3$ and $Bi_{0.5}Na_{0.02}Sb_{1.48-x}In_xTe_3$ ($x = 0.02$, 0.04, 0.06, 0.10, 0.20), respectively, They were charged into a quartz tube at 1×10^{-3} Pa. The elemental mixtures were melted at 1,073 K for 8 h using a rocking furnace to ensure the composition homogeneity, and then they were cooled to room temperature in the furnace. The obtained ingots were pulverized using the agate mortar in atmospheric environment. The sizes of obtained powders were controlled using the 300-mesh standard sieve. The powders were hot-pressed in the graphite dies under 60 MPa pressure at 753 K in a vacuum of 1×10^{-3} Pa for 30 min. Bulk disk-shaped pellets of Φ19.4 mm × 4 mm were fabricated by vacuum hot-pressing method.

The phase structure and cross-section morphology were characterized by X-ray diffraction (XRD, BRUKER, D8ADVANCE with Cu Kα radiation, $\lambda = 0.15406$ nm) and scanning electron microscopy (SEM, TESCAN, VEGA II LSU), respectively. The Seebeck coefficient S and the electrical resistivity ρ were measured simultaneously from 300 to 500 K via temperature differential and four-point probe methods in a custom-designed apparatus under vacuum circumstance. The electrical properties were measured perpendicular to the hot-pressing direction. The thermal conductivity κ was calculated from the thermal diffusivity (λ) parallel to the hot-pressing direction; the heat capacity (C_p) was obtained from LFA 457 laser flash apparatus. The thermal conductivity was calculated according to the equation: $\lambda = \kappa/(DC_p)$, where D is the density, which is calculated using the sample dimensions and mass. The figure of merit ZT was evaluated according to the equation: $ZT = S^2T/\rho\kappa$. All measurements were performed in the temperature range of 300–500 K.

3 Results and discussion

3.1 Microstructure

The XRD patterns of the $Bi_{0.5}Sb_{1.5}Te_3$ and the $Bi_{0.5}Na_{0.02}Sb_{1.48-x}In_xTe_3$ bulk samples are shown in Fig. 1. The XRD patterns of the $Bi_{0.5}Sb_{1.5}Te_3$ and the $Bi_{0.5}Na_{0.02}Sb_{1.48-x}In_xTe_3$ bulk samples prepared by HP are also consistent with rhombohedral $Bi_{0.5}Sb_{1.5}Te_3$ (JCPDS 49-1713) phase structure. The (00l) peaks including (006), (009), (0015) and (0018) become more intense in the diffraction spectrums. The diffraction spectrums of the bulk samples show the (00l) plane sharp peak with a preferentially oriented perpendicular to hot-pressing direction. The (00l)-oriented corresponds to the rhombohedral crystal structure of Bi_2Te_3 and Sb_2Te_3. We calculated the lattice constants of the samples according to the (006) and (015) peaks, using the following equation:

$$\frac{1}{d_{hkl}^2} = \frac{4}{3}\frac{h^2 + hk + k^2}{a^2} + \frac{l^2}{c^2} \quad (1)$$

The lattice parameters a of the $Bi_{0.5}Na_{0.02}Sb_{1.48-x}In_xTe_3$ ($x = 0.02$–0.20) gradually increase in comparison to those of the $Bi_{0.5}Sb_{1.5}Te_3$ in Table 1. Such a change corresponds to the proposed formation of substitutional defects by Na and In atoms, replacing Sb atoms in their lattice sites. The formation of structural defects by Na and In atoms in the cation sublattice should also be reflected in changes for the crystal lattice parameters. As the bonding radiuses of the Na and In atoms ($r_{Na} = 0.154$ nm, $r_{In} = 0.144$ nm) are bigger than that of the Sb atom ($r_{Sb} = 0.140$ nm), it is possible to expect a bigger volume of unit cell in the crystals containing substitutional defects of Na''_{Sb} and In''_{Sb}. It is evident that the volume of unit cell increases with the increase of In concentration. Based on the atomic radius of In and Na, one would expect the increase in the volume of unit cell.

Figure 2a, c indicates the SEM images of the bulk $Bi_{0.5}Sb_{1.5}Te_3$ and the $Bi_{0.5}Na_{0.02}Sb_{1.42}In_{0.06}Te_3$ alloys from sections parallel to hot-pressing direction. Compared with the SEM images of the $Bi_{0.5}Sb_{1.5}Te_3$, Fig. 2c shows a typical laminated structure composed of micro-nanolayers

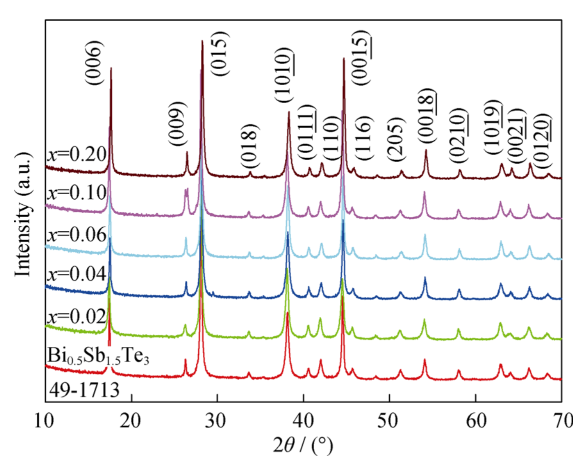

Fig. 1 XRD patterns of bulk $Bi_{0.5}Sb_{1.5}Te_3$ sample and $Bi_{0.5}Na_{0.02}Sb_{1.48-x}In_xTe_3$ samples

Table 1 Lattice parameters of the $Bi_{0.5}Sb_{1.5}Te_3$ and the $Bi_{0.5}Na_{0.02}Sb_{1.48-x}In_xTe_3$ alloys

Samples ($Bi_{0.5}Na_{0.02}$ $Sb_{1.48-x}In_xTe_3$)	*d*-spacing/nm	*a*/nm	*c*/nm	Volume of cell/nm^3
$Bi_{0.5}Sb_{1.5}Te_3$	0.506000 (006), 0.316672 (015)	0.428559	3.0360	0.48288
$x = 0.02$	0.505777 (006), 0.316957 (015)	0.429158	3.0347	0.48402
$x = 0.04$	0.507637 (006), 0.317452 (015)	0.429493	3.0458	0.48655
$x = 0.06$	0.508032 (006), 0.317571 (015)	0.429588	3.0482	0.48715
$x = 0.10$	0.507879 (006), 0.317607 (015)	0.429702	3.0473	0.48727
$x = 0.20$	0.508018 (006), 0.317621 (015)	0.429686	3.0481	0.48736

with the layer thicknesses of about 0.5 μm. Figure 2b and d indicates the SEM images of the bulk $Bi_{0.5}Sb_{1.5}Te_3$ and the $Bi_{0.5}Na_{0.02}Sb_{1.42}In_{0.06}Te_3$ alloys from sections perpendicular to hot-pressing direction. The polyhedral sheet-like grains are randomly arranged. The $Bi_{0.5}Sb_{1.5}Te_3$ sample is found to have few randomly spaced pores in Fig. 2b

3.2 Thermoelectric properties

The temperature dependence of the Seebeck coefficient, the electrical resistivity, the thermal conductivity and the *ZT* value for the bulk $Bi_{0.5}Sb_{1.5}Te_3$ and the $Bi_{0.5}Na_{0.02}Sb_{1.48-x}In_xTe_3$ ($x = 0.02$–0.20) alloys are shown in Fig. 3. As shown in Fig. 3a, all the samples exhibit the p-type semiconductor behavior. The Na and In dual doping results in substantial increase in Seebeck coefficient from 300 to 360 K. Compared with the undoped sample, Fig. 3b shows that the electrical resistivity of the Na and In dual-doping samples is larger ranging from 300 to 500 K. From the analysis of Table 1, it is also obvious that Na and In dual substitutions for Sb enlarge the volume of unit cell, which is a further proof that Na and In atoms enter the lattice and occupy the Sb sites. As shown in Fig. 3c, the thermal conductivity of the $Bi_{0.5}Na_{0.02}Sb_{1.48-x}In_xTe_3$ ($x = 0.02$,

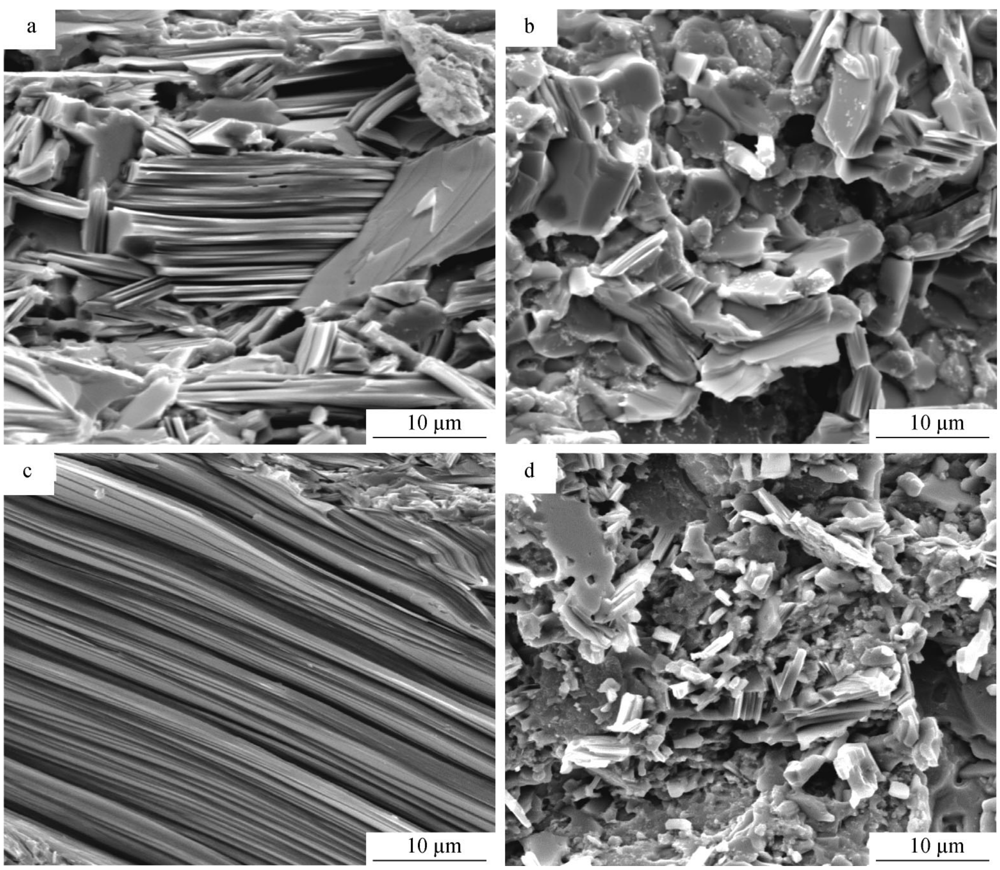

Fig. 2 SEM images of $Bi_{0.5}Sb_{1.5}Te_3$: **a** from sections parallel to hot-pressing direction and **b** from sections perpendicular to hot-pressing direction, SEM images of $Bi_{05}Na_{0.02}Sb_{1.42}In_{0.06}Te_3$: **c** from sections parallel to hot-pressing direction and **d** from sections perpendicular to hot-pressing direction

0.06) samples is lower than that of the undoped sample within the whole test temperature range. The alkali atoms tend to have soft rattling-type phonon modes, which results in low thermal conductivity in these materials [23]. With the increase in substitution fraction ($x = 0.04, 0.10, 0.20$), the thermal conductivity of the $Bi_{0.5}Na_{0.02}Sb_{1.48-x}In_xTe_3$ samples is larger than that of the undoped sample. For the $Bi_{0.5}Na_{0.02}Sb_{1.46}In_{0.02}Te_3$ specimen, a minimal thermal conductivity of 0.53 $W{\cdot}m^{-1}{\cdot}K^{-1}$ reaches at 320 K. Figure 3d shows temperature dependence of the *ZT* value. Expect from the $Bi_{0.5}$ $Na_{0.02}Sb_{1.42}In_{0.06}Te_3$ specimen, the *ZT* values of the other samples are lower than that of the $Bi_{0.5}Sb_{1.5}Te_3$ alloy from 300 to 500 K. Compared with the undoped sample, the $Bi_{0.5}Na_{0.02}Sb_{1.42}In_{0.06}Te_3$ sample shows higher *ZT* values from 300 to 380 K. A *ZT* of 1.26 is achieved at 300 K for the $Bi_{0.5}Na_{0.02}Sb_{1.42}In_{0.06}Te_3$, representing 26 % enhancement with respect to $ZT = 1.0$ of the undoped sample. The results confirm that appropriate Na and In dual partial substitutions for Sb are effective in enhancing thermoelectric figure of merit of $Bi_{0.5}Sb_{1.5}Te_3$ alloy.

To confirm effects of Na and In co-doping on thermoelectric properties of $Bi_{0.5}Sb_{1.5}Te_3$ alloy, thermoelectric properties of $Bi_{0.5}Sb_{1.5}Te_3$, Na-doped $Bi_{0.5}Sb_{1.5}Te_3$, In-doped $Bi_{0.5}Sb_{1.5}Te_3$ and Na–In co-doped $Bi_{0.5}Sb_{1.5}Te_3$ samples were investigated. Figure 4a shows that the Na and In co-doping results in an increase in Seebeck coefficient at near room temperature. Compared with the undoped sample, Fig. 4b shows that the electrical resistivity of the In-doping $Bi_{0.5}Sb_{1.5}Te_3$ has the lowest values from 300 to 500 K. However, the electrical resistivity of the Na-doped $Bi_{0.5}Sb_{1.5}Te_3$ samples is the highest within the whole test temperature range. As shown in Fig. 4c, the thermal conductivity of the co-doped $Bi_{0.5}Sb_{1.5}Te_3$ sample reduces effectively within the whole test temperature range. Figure 4d shows temperature dependence of the *ZT* value of the four samples. Compared with the undoped sample, the *ZT* values of the Na-doped $Bi_{0.5}Sb_{1.5}Te_3$ samples have an obvious decrease from 300 to 500 K. The *ZT* values of In-doped $Bi_{0.5}Sb_{1.5}Te_3$-sample are still lower than that of the $Bi_{0.5}Sb_{1.5}Te_3$ samples at near room temperature. The Na–In co-doped $Bi_{0.5}Sb_{1.5}Te_3$ samples have an increase in the *ZT* values from 300 to 375 K. It can be concluded that Na and In co-doping are effective in enhancing thermoelectric figure of merit of $Bi_{0.5}Sb_{1.5}Te_3$ alloy.

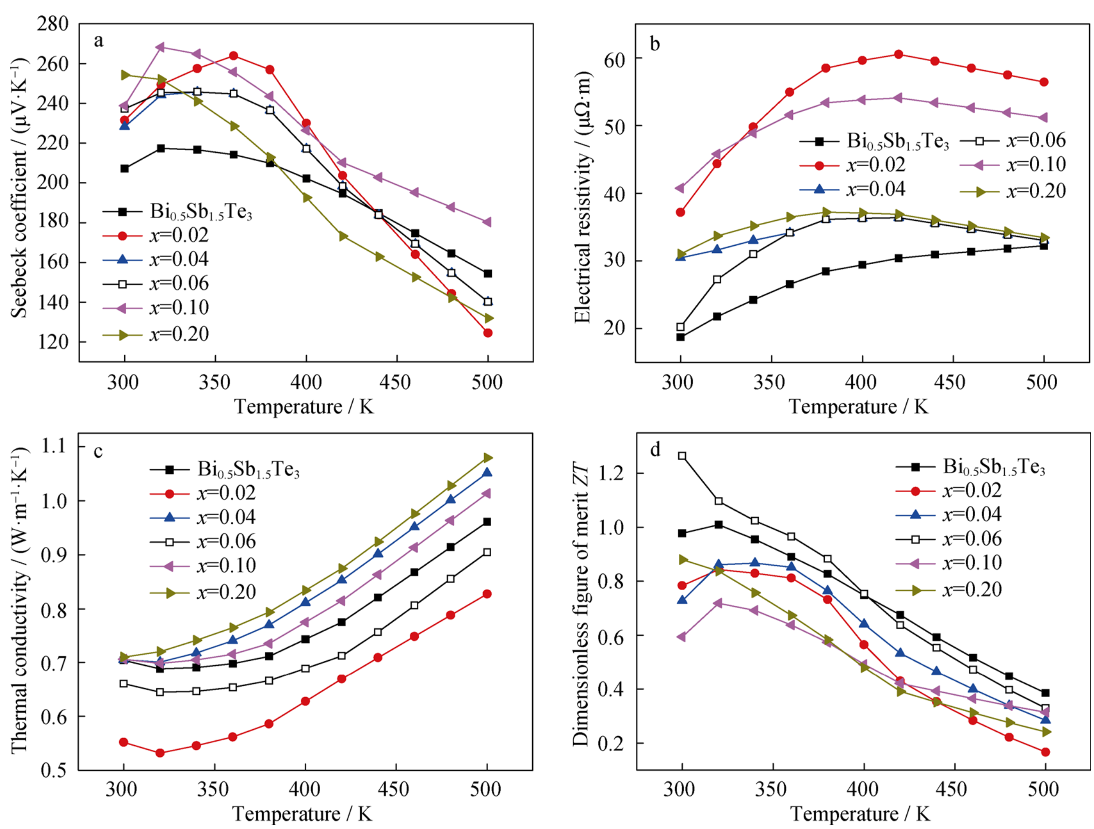

Fig. 3 Temperature dependence of **a** Seebeck coefficient, **b** electrical resistivity, **c** thermal conductivity and **d** *ZT* value of bulk $Bi_{0.5}Sb_{1.5}Te_3$ and $Bi_{0.5}Na_{0.02}Sb_{1.48-x}In_xTe_3$ ($x = 0.02$–0.20) alloys

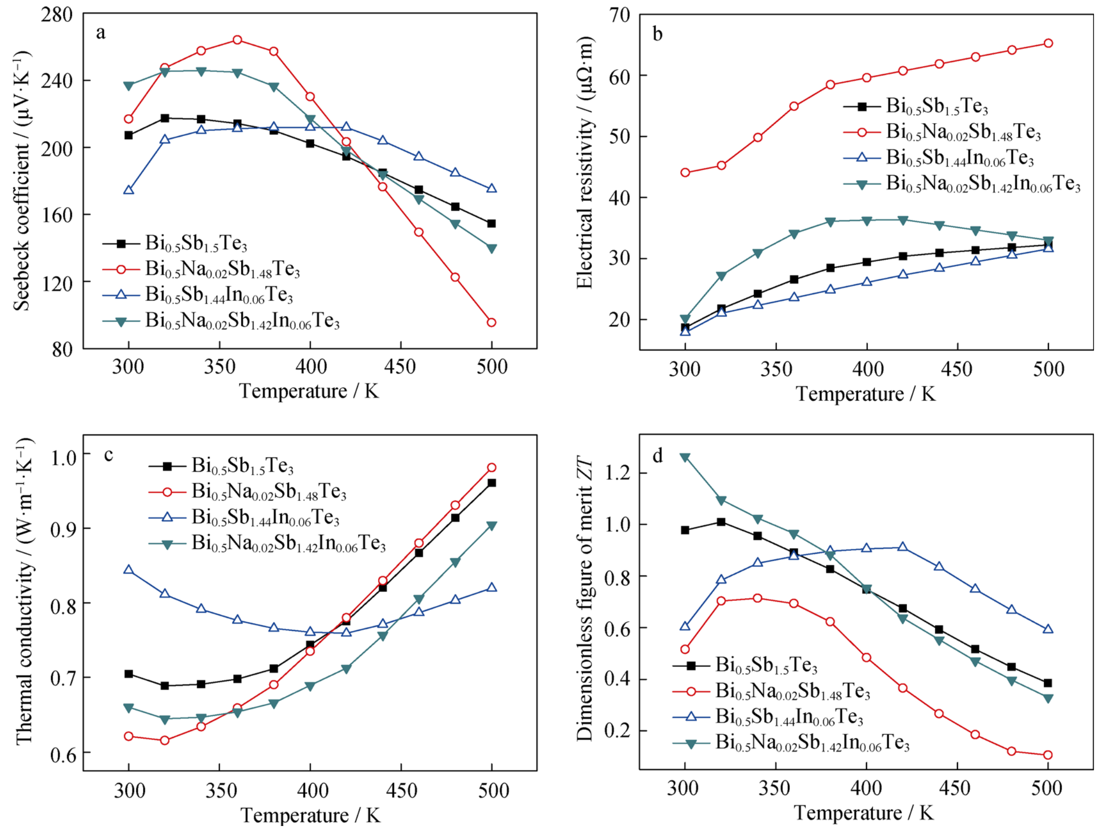

Fig. 4 Temperature dependence of **a** Seebeck coefficient, **b** electrical conductivity, **c** thermal conductivity and **d** *ZT* value of $Bi_{0.5}Sb_{1.5}Te_3$, $Bi_{0.5}Na_{0.02}Sb_{1.48}Te_3$, $Bi_{0.5}Sb_{1.44}In_{0.06}Te_3$ and $Bi_{0.5}Na_{0.02}Sb_{1.42}In_{0.06}Te_3$ samples

4 Conclusion

Thermoelectric properties of Na and In dual partial substitutions for Sb in the $Bi_{0.5}Na_{0.02}Sb_{1.48-x}In_xTe_3$ alloys were investigated. The $Bi_{0.5}Na_{0.02}Sb_{1.48-x}In_xTe_3$ samples result in substantial increase in Seebeck coefficient from 300 to 360 K. The electrical resistivity of the Na and In dual-doped samples is larger within the whole test temperature range. For the $Bi_{0.5}Na_{0.02}Sb_{1.46}In_{0.02}Te_3$ specimen, a minimal thermal conductivity of 0.53 $W \cdot m^{-1} \cdot K^{-1}$ is reached at 320 K. A *ZT* of 1.26 is achieved at 300 K for the $Bi_{0.5}Na_{0.02}Sb_{1.42}In_{0.06}Te$. Thermoelectric properties of $Bi_{0.5}Sb_{1.5}Te_3$, Na-doped $Bi_{0.5}Sb_{1.5}Te_3$, In-doped $Bi_{0.5}Sb_{1.5}Te_3$ and Na–In dual-doped $Bi_{0.5}Sb_{1.5}Te_3$ samples were also investigated. The results further confirm that Na and In dual partial substitutions for Sb are effective in enhancing thermoelectric figure of merit of $Bi_{0.5}Sb_{1.5}Te_3$ alloy.

Acknowledgments This study was financially supported by the National Natural Science Foundation of China (No. 51161009) and the Research Project of Jiangxi Provincial Education Department (No. GJJ13722 and GJJ11615).

References

[1] Tritt TM. Holey and unholey semiconductors. Science. 1999;283(5403):804.
[2] DiSalvo FJ. Thermoelectric cooling and power generation. Science. 1999;285(5428):703.
[3] Bell LE. Cooling, heating, generating power, and recovering waste heat with thermoelectric systems. Science. 2008;321(5895):1457.
[4] Dresselhaus MS, Chen G, Tang MY, Yang RG, Lee H, Wang DZ. New directions for low-dimensional thermoelectric materials. Adv Mater. 2007;19(8):1043.
[5] Poudel B, Hao Q. High-thermoelectric performance of nanostructured bismuth antimony telluride bulk alloys. Science. 2008;320(5876):634.
[6] Cao YQ, Zhao XB, Zhu TJ, Zhang XB, Tu JP. Syntheses and thermoelectric properties of Bi_2Te_3/Sb_2Te_3 bulk nanocomposites with laminated nanostructure. Appl Phys Lett. 2008;92(1):143106.
[7] Li YL, Jiang J, Xu GJ, Li W, Zhou LM, Li Y, Cui P. Synthesis of micro/nanostructured p-type $Bi_{0.4}Sb_{1.6}Te_3$ and its thermoelectric properties. J Alloys Compd. 2009;480(2):954.
[8] Xie WJ, Tang XF, Yan YG, Zhang QJ, Tritt TM. Unique nanostructures and enhanced thermoelectric performance of melt-spun BiSbTe alloys. Appl Phys Lett. 2009;94(2):102111.
[9] Kim DH, Kim C, Heo SH, Kim HY. Influence of powder morphology on thermoelectric anisotropy of spark-plasma-sintered Bi–Te-based thermoelectric materials. Acta Mater. 2011;59(1):405.

[10] Delaizir G, Bernard-Granger G, Monnier J, Grodzki R, Kim-Hak O, Szkutnik P, Soulier M, Saunier S, Goeuriot D, Rouleau O, Simon J, Godart C, Navone C. A comparative study of spark plasma sintering (SPS), hot isostatic pressing (HIP) and microwaves sintering techniques on p-type Bi_2Te_3 thermoelectric properties. Mater Res Bull. 2012;47(8):1954.
[11] Liu CJ, Lai HC, Liu YL, Liu LR. High thermoelectric figure-of-merit in p-type nanostructured (Bi, Sb)$_2$Te$_3$ fabricated via hydrothermal synthesis and evacuated-and-encapsulated sintering. J Mater Chem. 2012;22(11):4825.
[12] Yu FR, Xu B, Zhang JJ, Yu DL, He JL, Liu ZY. Structural and thermoelectric characterizations of high pressure sintered nanocrystalline Bi_2Te_3 bulks. Mater Res Bull. 2012;47(6):1432.
[13] André C, Vasilevskiy D, Turenne S, Masut RA. Increase in the density of states in n-type extruded $(Bi_{(1-x)}Sb_x)_2(Te_{(1-y)}Se_y)_3$ thermoelectric alloys. J Phys D. 2011;44(23):235401.
[14] Ajay SN, Zhao YY, Yu LG, Aik Michael KK, Dresselhaus MS, Xiong QH. Enhanced thermoelectric properties of solution grown $Bi_2Te_{3-x}Se_x$ nanoplatelet composites. Nano Lett. 2012;12(3):1203.
[15] Kim MY, Yeo YH, Park DH, Oh TS. Thermoelectric characteristics of the (Bi, Sb)$_2$(Te, Se)$_3$ nanocomposites processed with nanoparticle dispersion. Ceramics Int. 2012;38(S1):S529.
[16] Zhu YG, Shen HL, Chen HL. Effects of nano-TiO_2 dispersion on thermoelectric properties of $Co_4Sb_{11.7}Te_{0.3}$ composites. Rare Met. 2012;31(1):43.
[17] Gothard N, Ji X, He J, Tritt TM. Thermoelectric and transport properties of n-type Bi_2Te_3 nanocomposites. J Appl Phys. 2008;103(5):054314.
[18] Chen C, Zhang BP, Liu DW, Ge ZH. Thermoelectric properties of $Cu_yBi_xSb_{2-x-y}Te_3$ alloys fabricated by mechanical alloying and spark plasma sintering. Intermetallics. 2012;25(6):131.
[19] Ceyda Yelgel Ö, Srivastava GP. Thermoelectric properties of n-type $Bi_2(Te_{0.85}Se_{0.15})_3$ single crystals doped with CuBr and SbI_3. Phys Rev B. 2012;85(12):125207.
[20] Soliman LI, Nassary MM, Shaban HT, Salwa AS. Influence of Se on the electron mobility in thermal evaporated $Bi_2(Te_{1-x}Se_x)_3$ thin films. Vacuum. 2010;85(3):358.
[21] Cui JL, Xue HF, Xiu WJ, Mao LD, Ying PZ, Jiang L. Crystal structure analysis and thermoelectric properties of p-type pseudo-binary $(Al_2Te_3)_x$–$(Bi_{0.5}Sb_{1.5}Te_3)_{1-x}$ alloys prepared by spark plasma sintering. J Alloys Compd. 2008;460(1–2):426.
[22] Du BL, Li H, Tang XF. Enhanced thermoelectric performance in Na-doped p-type nonstoichiometric $AgSbTe_2$ compound. J Alloys Compd. 2011;509(5):2039.
[23] Chung DY, Lordanidis L, Choi KS, Kanatzidis MG. Complex chalcogenides as thermoelectric materials: a solid state chemistry approach. Bull Korean Chem. 1998;19(12):1283.